

Supercritical CO₂-Mediated Intercalation of PEO in Clay

Qian Zhao[†] and Edward T. Samulski^{*,†,‡}

Curriculum in Applied and Materials Sciences,
University of North Carolina at Chapel Hill, Chapel Hill,
North Carolina 27599-3290, and Department of Chemistry,
University of North Carolina at Chapel Hill,
Chapel Hill, North Carolina 27599-3290

Received July 9, 2003

Revised Manuscript Received August 1, 2003

Introduction. Polymer/clay nanocomposites prepared by a variety of methods that embed these inorganic nanolayers to a polymer host have been actively studied in recent years as these materials exhibit dramatic, concurrent improvements in many properties.¹ Typical preparation methods include in-situ polymerization, solution intercalation, and melt intercalation, among which solution intercalation has been known for over a century and has proved to be one of the most successful methods of incorporating delaminated clay into polymers.² Many polymers have been intercalated into clay via this method: Examples include water-soluble polymers such as poly(ethylene oxide) and poly(vinyl alcohol)^{3,4} and organic solvent-soluble polymers such as high-density polyethylene,⁵ poly(L-lactide),⁶ etc. Despite many laboratory successes with solution intercalation, its application on an industrial scale is still hindered by two major problems: (1) involvement of large quantities of aqueous/organic solvent; (2) a limited number of solvent/polymer pairs available for polymer dissolution and subsequent intercalation.

During the past decade, supercritical carbon dioxide (sc CO₂) has attracted a great deal of attention as an “environmentally benign, inexpensive, and nonflammable alternative” solvent for polymer synthesis and processing.^{7,8} The low viscosity, near-zero surface tension, relative chemical inertness, and high diffusivity of sc CO₂ results in negligible competitive adsorption with guest molecules on the host substrate and therefore facilitates solute transfer relative to normal solvents. Furthermore, since CO₂ is a gas at ambient conditions, the tedious drying procedure associated with conventional liquid solvents is circumvented, and the product is free of residual solvent upon depressurization.

These unique properties of sc CO₂ have been exploited to prepare polymer blends.^{9–12} The usual method employs sc CO₂ as a swelling agent to facilitate the diffusion of a guest monomer into a CO₂-swollen polymer matrix. Subsequent polymerization develops a blend of submicron phase-separated polymers. Recently, an in-situ polymerization method used sc CO₂ as a processing aid to achieve a uniform reinforcement distribution in a polymer/clay composite at high clay loading (~40 wt %).¹³

Intercalation of unreactive small molecules into layered clay in the presence of sc CO₂ has also been

described.^{14–16} In a recent report, Isii et al compared sc CO₂ with other organic solvents for the intercalation of the dye 4-phenylazoaniline into a pillared clay.¹⁷ They found sc CO₂ was a superior adsorption medium for both the equilibrium adsorptivity and the adsorption kinetics of the dye intercalation. They attributed the superiority of CO₂ to the lower dye solubility, the solvent's higher diffusivity, and its much lower viscosity relative to normal liquids. Although most technologically important polymers are relatively insoluble in CO₂, Garcia-Leiner and Lesser¹⁸ recently reported that sc CO₂ stimulates intercalation during the foaming of melt-extruded polyethylene and polyesters.

In this Communication, we present unambiguous evidence for sc CO₂-mediated intercalation of a polymer into silicate nanolayers. We chose PEO/Na–montmorillonite as a model system since it is a well-studied system for both solution intercalation and melt intercalation.^{3,19,20} Conventional solution intercalation is limited to certain polymer/solvent pairs, in which the polymer is soluble and the silicate layers are swellable.²¹ Here, sc CO₂ intercalation is qualitatively different from conventional solution intercalation as PEO is not soluble in sc CO₂. Rather, PEO is reversibly plasticized by sc CO₂, depressing its melting point and effectively facilitating a meltlike intercalation.

Materials and Methods. a. Materials. Sodium montmorillonite (MMT) was obtained from Gelest, Inc., and used as received. Poly(ethylene oxide) of average molecular weight $M_w = 1 \times 10^5$ was supplied by Aldrich Chemical Co., Inc.

b. Methods. Composites were fabricated in CO₂ in a 2.5 mL, high-pressure cell equipped with sapphire windows that allow visual observation of the mixture. PEO and MMT power mixtures were weighed into the cell according to designated ratios. An Isco automatic syringe pump (model 260D) was used to pressurize the cell with CO₂ to 193 ± 7 bar, and the mixture was heated to 48 °C with a heating tape wrapped around the cell. After the desired pressure and temperature were reached, the intercalation was allowed to proceed with stirring for 1 day. At the end of the intercalation period, the cell was cooled and CO₂ was slowly vented from the cell. The final product was taken out and dried at room temperature in a vacuum oven overnight, and the resultant materials stored in a desiccator. Powder X-ray diffraction (XRD) data between $2\theta = 2^\circ$ and $2\theta = 10^\circ$ were collected on a Rigaku multiflex diffractometer using Cu K α radiation (40 kV, 40 mA) at 0.5°/min. Thermogravimetric analysis (TGA) and differential scanning calorimetry (DSC) were performed using a Perkin-Elmer Pyris 1 TGA and DSC system. For the DSC measurement, samples weighing 5–10 mg were loaded into an aluminum pan, and the sample chamber was purged with argon prior to heating at 10°/min. For TGA measurement, approximately 10 mg of samples was loaded in an open ceramic crucible and heated in an argon atmosphere at a heating rate of 10°/min.

Results and Discussion. The efficacy of CO₂-mediated intercalation is shown by the expansion of (001) d spacing of the PEO/MMT composites. An increase in the “gallery” spacing is displayed in Figure 1. The (001) peak of the PEO/MMT composite shifts from 1.20 nm in the pristine MMT (the gallery contains a monolayer

[†] Curriculum in Applied and Materials Sciences.

[‡] Department of Chemistry.

* To whom correspondence should be addressed: e-mail et@unc.edu.

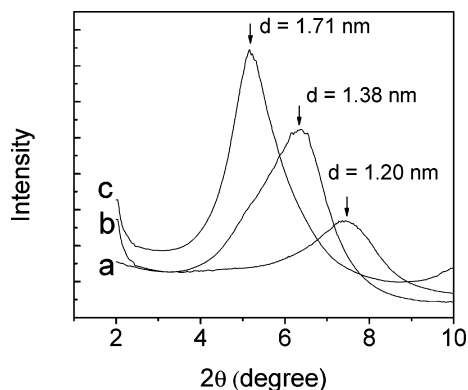


Figure 1. XRD patterns of PEO/MMT nanocomposites prepared by sc CO₂-mediated intercalation: (a) pristine MMT, (b) PEO content 9.1%, and (c) PEO content 16.7%.

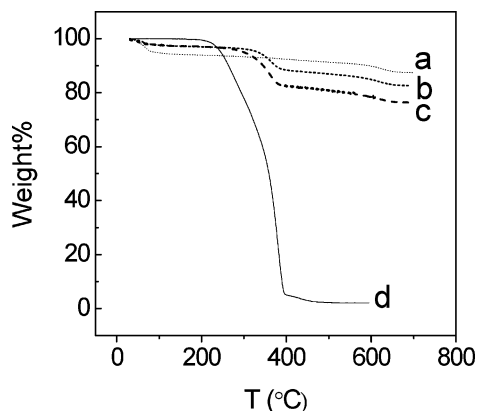


Figure 2. TGA curves of PEO/MMT under an argon atmosphere: (a) pristine MMT, (b) PEO content 9.1%, (c) PEO content 16.7%, and (d) pure PEO.

of water) to 1.71 nm at a PEO content of 16.7%. This change in the d spacing corresponds to a gallery expansion of 0.75 nm, since anhydrous MMT is known to have a 0.96 nm basal plane spacing.³ At a PEO content of 9.1%, a lower d spacing is observed ($d = 1.38$ nm), corresponding to a gallery expansion of 0.42 nm. These results are similar to aqueous solution intercalation results by Shen and co-workers using PEO in water.¹⁹ They reported a smaller gallery expansion (from 0.47 to 0.53 nm) when PEO was less than 15% and a larger gallery expansion (0.83 nm) for PEO contents $\geq 15\%$.

Figure 2 shows the TGA curves of pristine MMT, PEO/MMT nanocomposites (PEO content is 9.1% and 16.7%), and pure PEO obtained under an argon atmosphere at 10°/min. The TGA profile of pristine MMT (curve a) shows two typical weight loss transitions. The one below 100 °C is due to dehydration of physisorbed water molecules in the gallery interlayer, and the other around 630 °C is due to dehydroxylation of the aluminosilicate structure. As shown in curves b and c, the intercalated PEO in the MMT composites begins to decompose around 300 °C, a temperature much higher than the decomposition temperature of pure PEO (around 200 °C, curve d). The higher decomposition temperature is frequently attributed to the barrier characteristics of clay nanolayers which mandate a tortuous pathway for volatile degradation products,²² but there may be specific clay–PEO interactions that also increase the thermal stability. The major weight loss for the two composites occurs around 400 °C and corresponds to complete elimination of PEO, in agree-

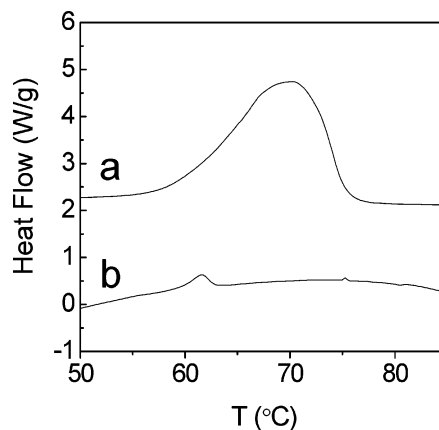


Figure 3. DSC traces of PEO and PEO/MMT composite: (a) pure PEO; (b) PEO content 16.7%.

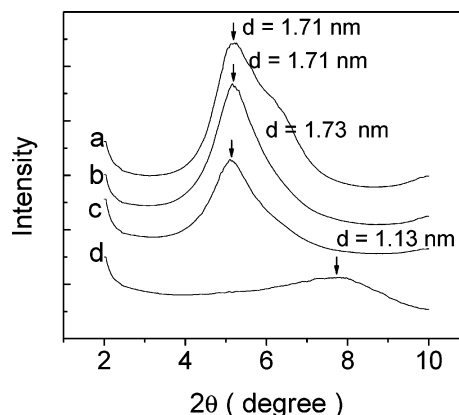


Figure 4. XRD patterns of PEO/MMT (PEO content 16.7%) nanocomposites from different solvents: (a) water; (b) sc CO₂; (c) methanol; (d) *n*-hexane

ment with the initial targeted organic contents (PEO = 9.1% and 16.7%).

Further evidence for intercalation is obtained from differential scanning calorimetry (DSC) analysis of the melting peak of PEO. As shown in Figure 3, the endotherm peak area of the PEO melting in the MMT/PEO composite is significantly reduced after CO₂-mediated intercalation and suggests that most of the PEO resides in the MMT galleries. The apparent shift in the melting transition has been attributed to water incorporation into the PEO crystals²⁰ and/or imperfect crystals in the constraining environment of the interlamellar gallery.²³

Solution intercalation with water, methanol, and *n*-hexane under the same conditions (PEO content 16.7%, reacting for 1 day at 48 °C) was also investigated for comparison with the CO₂-mediated intercalation. In Figure 4 the XRD patterns of both water and methanol intercalation are similar; the dominant peak (~ 1.7 nm) indicates successful intercalations using these solvents. This is not surprising since water and methanol are both good solvents for PEO, and both have proved to be effective intercalation solvents according to previous reports.^{3,19} By contrast, *n*-hexane is a nonpolar solvent and does not dissolve PEO, and PEO cannot intercalate into MMT; the (001) peak is unchanged from that of pristine clay, as is shown in curve d of Figure 4. Supercritical CO₂ is also a nonpolar solvent, yet it shows intercalation comparable to that of the polar solvents water and methanol.

To gain a better appreciation on the effect of CO₂ in PEO intercalation, we studied the swelling behavior of PEO using a custom-made, high-pressure minicell in conjunction with optical microscopy. Preliminary qualitative observations show that, even at room temperature, exposure to CO₂ at 103 bar causes the initial sharply defined semicrystalline PEO thin film melt, and all of its edges become rounded. Upon depressurization, the rounded swollen film foams and bubbles are visible. It is known that CO₂ can swell and assist melting of certain polymers,²⁴ and low molecular weight ($M_w = 1500$) PEG was recently reported to be in the molten state at 40 °C under CO₂ pressure.²⁵

Concluding Remarks. Polymer intercalation in solution has been long thought to be an entropy-driven process, in which the translational entropy gained by desorption of solvent molecules from the gallery interlayer compensates the entropy decrease of the confined polymer chains.² However, this mechanism is probably not applicable to sc CO₂-mediated intercalation. As anticipated, thermogravimetric analysis (TGA) shows that after MMT is incubated in CO₂ under the same conditions (24 h, 48 °C), the MMT has about the same weight loss in the range between 50 and 100 °C as the original untreated MMT. There appears to be no release of water from the host gallery by the CO₂ treatment. Further evidence from the PEO swelling experiment corroborates the strong plasticizing effect of CO₂ on PEO and suggests that the intercalation mechanism is similar to that in polymer melts. Therefore, the CO₂-mediated intercalation must be an enthalpically driven process, deriving from a favorable interaction between MMT and PEO, one that is sufficient to overcome the entropy penalty for the confinement of PEO. That is, polar interactions between clay and polymer drive intercalation.²⁶

In summary, we have successfully intercalated PEO into clay via a CO₂-mediated process. The resultant nanocomposites have been characterized by XRD, TGA, and DSC and showed results comparable to those achieved with conventional solution intercalation. While conventional solution intercalation is based on a solvent system in which the polymer is soluble and driven primarily by the entropy gained by desorption of solvent molecules within the clay gallery, the CO₂-mediated intercalation appears to be an enthalpically driven process, one which is facilitated by a reversible CO₂ plasticizing effect. Hence, CO₂-mediated intercalation mainly depends on the nature of the polymer–clay interactions rather than the solubility of the polymer. This suggests that, by judiciously choosing plasticizable polymers that have propensity for interacting with clay, the CO₂-mediated process may expand the range of polymer/clay nanocomposites.

Acknowledgment. This work was supported in part by NASA Grant NAG-1-2301 and used NSF–STC shared equipment facilities under Agreement No. CHE-9876674. We thank Dr. Peter S. White for assistance in XRD measurements, Prof. O. Zhou for the use of TGA and DSC instrumentation, and Prof. J. DeSimone for helpful discussions.

References and Notes

- (1) LeBaron, P. C.; Wang, Z.; Pinnavaia, T. J. *Appl. Clay Sci.* **1999**, *15*, 11–29.
- (2) Theng, B. K. G. *Formation and Properties of Clay-Polymer Complexes*; Elsevier Scientific Pub. Co.: New York, 1979.
- (3) Wu, J. H.; Lerner, M. M. *Chem. Mater.* **1993**, *5*, 835–838.
- (4) Ogata, N.; Kawakage, S.; Ogihara, T. *J. Appl. Polym. Sci.* **1997**, *66*, 573–581.
- (5) Joen, H. G.; Jung, H.-T.; Lee, S. W.; Hudson, S. D. *Polym. Bull.* **1998**, *41*, 107–113.
- (6) Ogata, N.; Jimenez, G.; Kawai, H.; Ogihara, T. *J. Polym. Sci., Part B: Polym. Phys.* **1997**, *35*, 389–396.
- (7) Shaffer, K. A.; DeSimone, J. M. *Trends Polym. Sci.* **1995**, *3*, 146–153.
- (8) Canelas, D. A.; DeSimone, J. M. *Adv. Polym. Sci.* **1997**, *133*, 103–140.
- (9) Liu, Z. M.; Wang, J. Q.; Dai, X. H.; Han, B. X.; Dong, Z. X.; Yang, G. Y.; Zhang, X. L.; Xu, J. *J. Mater. Chem.* **2002**, *12*, 2688–2691.
- (10) Hayes, H. J.; McCarthy, T. J. *Macromolecules* **1998**, *31*, 4813–4819.
- (11) Watkins, J. J.; McCarthy, T. J. *Macromolecules* **1994**, *27*, 4845–4847.
- (12) Kung, E.; Lesser, A. J.; McCarthy, T. J. *Macromolecules* **1998**, *31*, 4160–4169.
- (13) Zerda, A. S.; Caskey, T. C.; Lesser, A. J. *Macromolecules* **2003**, *36*, 1603–1608.
- (14) Shi, T. P.; Yao, K.; Nishimura, S.; Imai, Y.; Yamada, N.; Abe, E. *Chem. Lett.* **2002**, 440–441.
- (15) Yoda, S.; Sakurai, Y.; Endo, A.; Miyata, T.; Otake, K.; Yanagishita, H.; Tsuchiya, T. *Chem. Commun.* **2002**, 1526–1527.
- (16) Ishii, R.; Wada, H.; Ooi, K. *Chem. Commun.* **1998**, 1705–1706.
- (17) Ishii, R.; Wada, H.; Ooi, K. *J. Colloid Interface Sci.* **2002**, *254*, 250–256.
- (18) Garcia-Leiner, M.; Lesser, A. J. *Polym. Mater. Sci. Eng.* **2003**, *88*, 92–93.
- (19) Shen, Z. Q.; Simon, G. P.; Cheng, Y. B. *Polymer* **2002**, *43*, 4251–4260.
- (20) Vaia, R. A.; Vasudevan, S.; Krawiec, W.; Scanlon, L. G.; Giannelis, E. P. *Adv. Mater.* **1995**, *7*, 154–156.
- (21) Greenland, D. G. *J. Colloid Sci.* **1963**, *18*, 647–664.
- (22) Burnside, S. D.; Giannelis, E. P. *Chem. Mater.* **1995**, *7*, 1597–1600.
- (23) Shen, Z. Q.; Simon, G. P.; Cheng, Y. B. *Polym. Eng. Sci.* **2002**, *42*, 2369–2382.
- (24) Zhang, Z. Y.; Handa, Y. P. *Macromolecules* **1997**, *30*, 8505–8507.
- (25) Heldebrant, D. J.; Jessop, P. G. *J. Am. Chem. Soc.* **2003**, *125*, 5600–5601.
- (26) Vaia, R. A.; Giannelis, E. P. *Macromolecules* **1997**, *30*, 8000–8009.

MA0349682